



ELSEVIER

Available online at www.sciencedirect.com

SCIENCE @ DIRECT®

Journal of Magnetism and Magnetic Materials 288 (2005) 168–172



www.elsevier.com/locate/jmmm

High-frequency electron magnetic resonance and magnetic studies of ferrihydrite nanoparticles and evidence of a phase transition

A. Punnoose^{a,*}, M.S. Seehra^b, J. van Tol^c, L.C. Brunel^c

^aDepartment of Physics, Boise State University, Boise, ID 83725-1570, USA

^bDepartment of Physics, West Virginia University, Morgantown, WV 26506, USA

^cNational High Magnetic Field Laboratory, Center for Interdisciplinary Magnetic Resonance, Florida State University, Tallahassee, FL 32310, USA

Received 28 May 2004; received in revised form 31 August 2004

Available online 2 October 2004

Abstract

Temperature variations (300–4 K) of the electron magnetic resonance (EMR) spectra of ferrihydrite ($\text{FeOOH} \cdot n\text{H}_2\text{O}$) nanoparticles of size ≈ 5 nm are reported at the frequencies of $\nu = 190.62$ and 285.93 GHz. The EMR line at 300 K, occurring near $g \approx 2$, broadens and shifts to lower fields with decreasing T for $T > T_s = 30$ K. For $T < T_s$, the trend reverses in that the line narrows and shifts to higher fields. In magnetic studies, the coercivity H_c is maximum at T_s (approaching zero at the blocking temperature $T_B \approx 65$ K) with the appearance of exchange bias H_E for $T < T_s$. The magnetic viscosity is also maximum near T_s , approaching zero above T_B . These observations lead to the suggestion that T_s represents a phase transition to a new magnetically ordered state, with spin-glass-like ordering of the uncompensated Fe^{3+} spins.

© 2004 Elsevier B.V. All rights reserved.

PACS: 75.50.Tt; 75.50.Ee; 75.75.+a; 75.20.-g

Keywords: Nanoparticles; Superparamagnetism; High frequency EPR

Magnetic properties of materials in reduced dimensions (thin films, nanowires, nanoparticles or quantum dots) differ significantly from those of their bulk counterparts [1]. Structural and mag-

netic properties of ferrihydrite (FHYD) nanoparticles, with the general formula $\text{FeOOH} \cdot n\text{H}_2\text{O}$ and typical particle size ≈ 5 nm, have attracted a great deal of attention in recent years [2–5]. From the recent magnetic and neutron diffraction studies of FHYD, it is known that the blocking temperature $T_B \approx 65$ K as determined from DC

*Corresponding author. Tel.: 208 426 2268; fax: 208 426 4330.
E-mail address: apunnoos@boisestate.edu (A. Punnoose).

magnetic susceptibility (χ) measurements and the Néel temperature $T_N \simeq 350$ K. For $T > T_B$, χ vs. T data can be explained reasonably well by superparamagnetism, with a magnetic moment $\mu_p \simeq 300 \mu_B$ per particle due to uncompensated Fe^{3+} surface spins [3–5]. In electron magnetic resonance (EMR) studies carried out at 9.24 GHz, the observed line at $g \simeq 2$ (due to the uncompensated Fe^{3+} spins) broadens and shifts rapidly to lower fields as T is lowered from 300 K so that the line could not be followed for $T < 80$ K [6]. Here we report new EMR studies of FHYD from 300 to 4 K using the high frequencies of 190.62 and 285.93 GHz which were carried out at the National High Magnetic Field Laboratory. The new results show that the room temperature EMR line at $g \simeq 2$ continues to broaden and shift to lower fields as T decreases towards 30 K. For $T < 30$ K, the EMR parameters reverse in trend that the line narrows and shifts to higher fields with decreasing T . In magnetic studies, the coercivity H_C and magnetic viscosity S are maximum near T_s , with the appearance of exchange bias H_E for $T < T_s$. From these results, it is argued that a transition to a new magnetically ordered state occurs at T_s . This transition involves the uncompensated Fe^{3+} spins responsible for the EMR signal. The magnetic viscosity studies suggest spin-glass-like ordering somewhat similar to the observations in $\gamma\text{-Fe}_2\text{O}_3$ [7–9]. Details of these results are presented below.

Temperature variations of the resonance field H_r and the linewidth ΔH are shown in Fig. 1 for the operating frequencies of $\nu = 190.62$ and 285.93 GHz. For reference, the calculated values of H_r for $g = 2$ are 6.8136 T (10.22 T) for $\nu = 190.62$ GHz (285.93 GHz), close to the experimental values at room temperature. With decreasing T , H_r decreases and ΔH increases, as reported earlier for $\nu = 9.24$ GHz [4], although in the latter case, the line could not be followed for $T < 80$ K. At the higher operating frequencies, and consequently higher resonance fields, the EMR line could be followed down to 5 K. The two new results from this work are as follows: (i) below $T_B \simeq 65$ K, there is a hysteresis in the magnitudes of H_r and ΔH with increasing and decreasing fields. The magnitudes of H_r and ΔH shown in Fig. 1 are the average values; (ii) for $T < T_s$ ($\simeq 30$ K), the trend

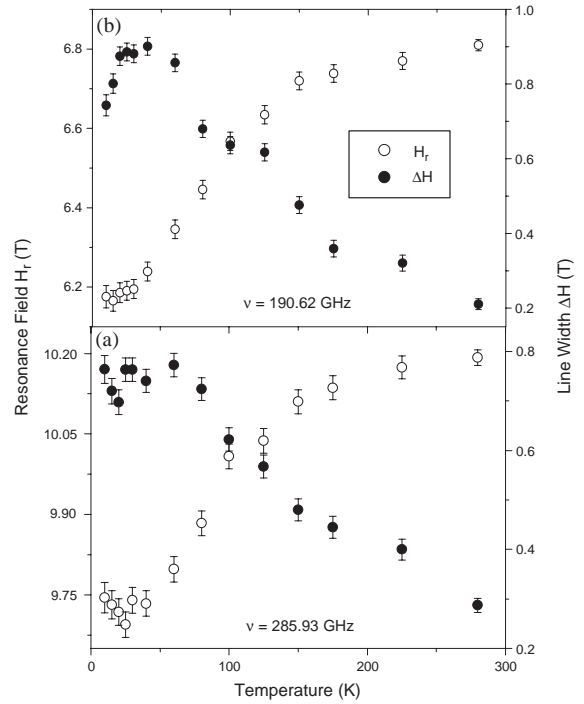


Fig. 1. Temperature variations of the resonance field H_r and the linewidth ΔH measured at the operating frequencies of (a) 285.93 GHz and (b) 190.62 GHz.

in the variations of H_r and ΔH with temperature reverses in that H_r increases and ΔH decreases with decrease in temperature. It is believed that for $T < T_s$, the system undergoes a phase transition to a different magnetically ordered state. The magnetic studies reported later in this paper provides additional support for this transition.

The data in Ref. [6] was interpreted in terms of the model of Nagata and Ishihara [10] in which δH_r , representing change in the resonance field from the $g = 2$ value, and the linewidth ΔH are related to the anisotropy in non-spherical particles with a statistical distribution of sizes and shapes, leading to

$$\delta H_r \propto (\Delta H)^n, \quad (1)$$

where $n = 2$ (3) is predicted for partially (randomly) oriented particles. For our samples, transmission electron microscopy studies reported in a recent paper [5], showed a Gaussian size distribution of the particles with the following

characteristics: mean size = 5 nm; root mean square deviation = 1.5 nm; and ellipsoidal shape with aspect ratio ≈ 1.2 . In our earlier 9.24 GHz studies in FHYD, and Ni- and Si-doped FHYD [6], the data yielded $n \approx 3$ in the limited temperature range possible in these experiments. To see whether the new data is also consistent with $n = 3$ in the extended temperature range possible with the high-frequency experiments, in Fig. 2 we plot $\log(\delta H_r)$ against $\log(\Delta H)$, where the data taken at 9.24 and 190.62 GHz data are included. The new high-frequency data for 190.62 and 285.93 GHz yields the slope $n \sim 2.5$, as compared to $n \sim 3$ for the 9.24 GHz data. Also for $T < T_s$, the data show a knee as expected from the behavior shown in Fig. 1. The slightly lower values of n for the high-frequency experiments may be due to additional alignment of the particles under the high fields needed to observe resonance at such high frequencies.

The changes in the line width ΔH of the EMR line with microwave frequency are shown in Fig. 3 at three temperatures viz. $T = 5, 70$ and 285 K. For $T = 70$ and 285 K, $T > T_B$ and ΔH increases with increase in ν in a non-linear manner, whereas a systematic trend is not observed for $T = 5$ K. To

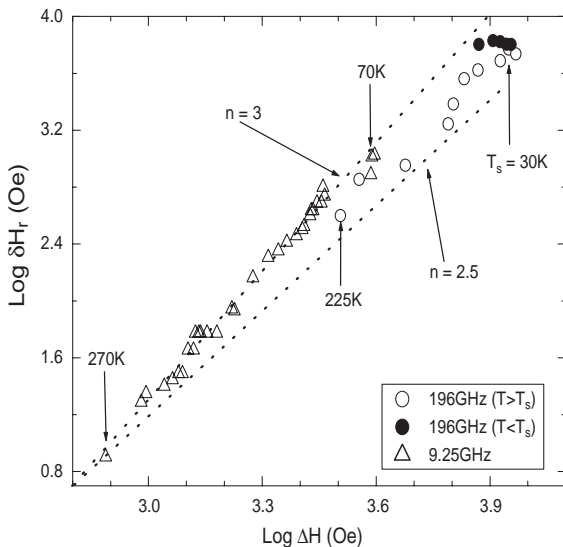


Fig. 2. Plot of $\log(\delta H_r)$ against $\log(\Delta H)$ using the data taken at frequencies of 9.24 and 190.62 GHz. Dotted lines indicate positions corresponding to $n = 3$ and 2.5 in Eq. (1).

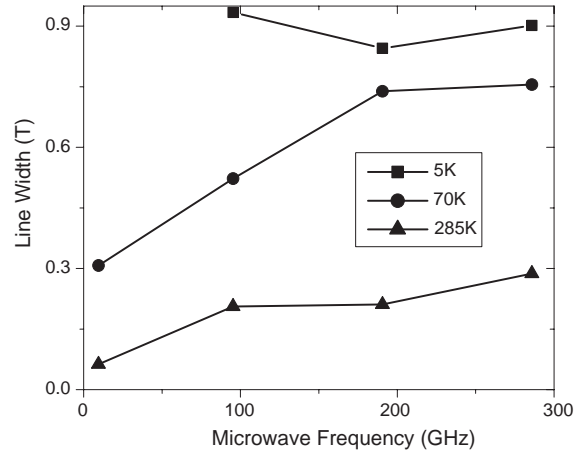


Fig. 3. Changes in the line width ΔH of the EMR line with microwave frequency measured at 5, 70 and 285 K. Lines connecting the points are drawn for clarity.

understand the data for $T > T_B$, we note that the dominant contribution to magnetic anisotropy and hence ΔH comes from the shape anisotropy and the resulting demagnetizing field, the latter being proportional to the magnetization M . However, M varies with H in a non-linear way following the modified Langevin behavior [3–5]:

$$M = M_0 \mathcal{L}(\mu_p H / k_B T) + \chi_a H, \quad (2)$$

where M_0 is the saturation magnetization, μ_p is the average magnetic moment per particle, χ_a is the AF susceptibility, k_B is the Boltzmann constant and $\mathcal{L}(x) = \coth(x) - (1/x)$ is the Langevin function. According to Eq. (2), M increases with increase in H and decrease in T . The changes in ΔH with ν (and hence with H) are in qualitative agreement with the predictions of Eq. (2). For $T = 5$ K, which is well below the T_B and T_s , Eq. (2) is not valid and the above argument cannot be applied.

To understand the nature of the transition at $T_s \approx 30$ K, we carried out additional magnetic measurements. In Fig. 4, we show the temperature variation of the coercivity H_C and loop shift or exchange bias H_E measured under zero-field cooled (ZFC) conditions and for the sample cooled from 300 K to the measuring temperature in $H = 50$ kOe (FC). Under FC, the hysteresis loop is shifted to the negative field side by H_E , and

H_c is lowered for $T < T_s$. The results in Fig. 4 show that although H_c goes to zero only at T_B , $H_c(\text{FC}) < H_c(\text{ZFC})$ and $|H_E| > 0$ for $T < T_s$. These results are similar to those reported for $\gamma\text{-Fe}_2\text{O}_3$ nanoparticles below the spin-glass transition at 40 K [7]. Thus, the transitions at T_s in FHYD may

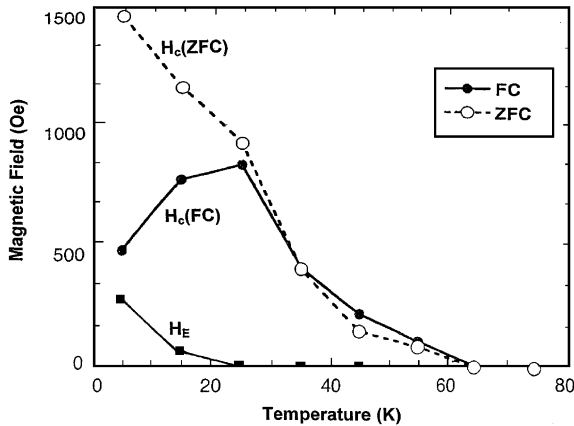


Fig. 4. Temperature variation of coercivity H_c and exchange bias H_E measured under zero-field cooled (ZFC) and field-cooled (FC) conditions. Lines connecting the points are drawn for clarity.

involve spin-glass ordering of the uncompensated Fe^{3+} spins.

To get further insight into the nature of the magnetic state below T_s , we measured the magnetic viscosity S as a function of temperature. The definition of S for a complex system with a distribution of barrier heights is usually written as [11,12]

$$M(t) = M(t_0)[1 - S \ln(t/\tau_0)], \quad (3)$$

where τ_0 is a constant and $M(t_0)$ is the magnetization at an initial time t_0 . For our experiments, we cooled the sample in $H_1 = 100$ Oe to the measuring temperature, then switched the field to $H_2 = -100$ Oe, followed by measurements of M as a function of time in 60 s intervals. Plots of M as a function of $\ln t$ are shown in Fig. 5 for different temperatures. The slope of the curves $= -|M(t_0)| S$ and hence, S can be evaluated. The plot of measured S for different temperatures given in Fig. 6 shows S peaking near T_s and S approaches zero at $T = T_B$. The maximum in S and $H_c(\text{FC})$ in Fig. 5 are most likely related to the same mechanism.

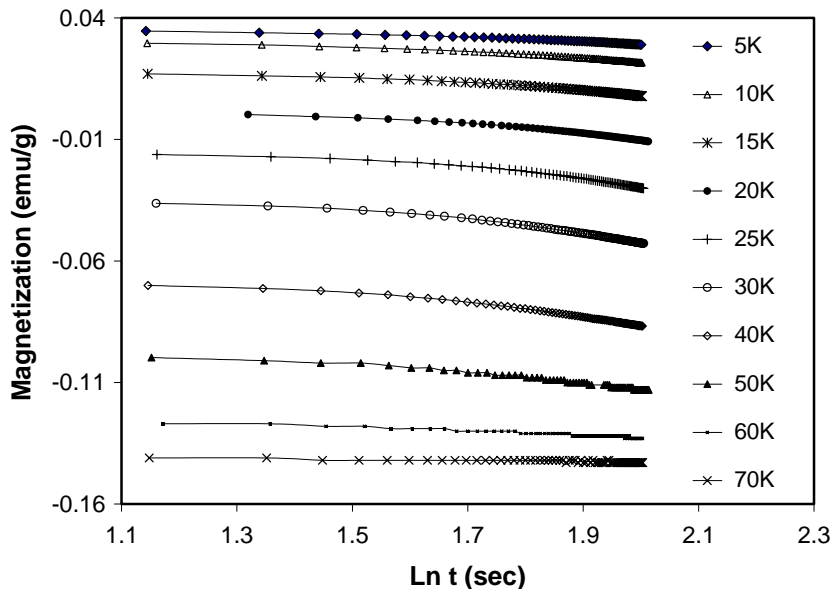


Fig. 5. Plots of the sample magnetization $M(t)$ as a function of $\ln t$ measured at different temperatures. Lines connecting the points are drawn for clarity.

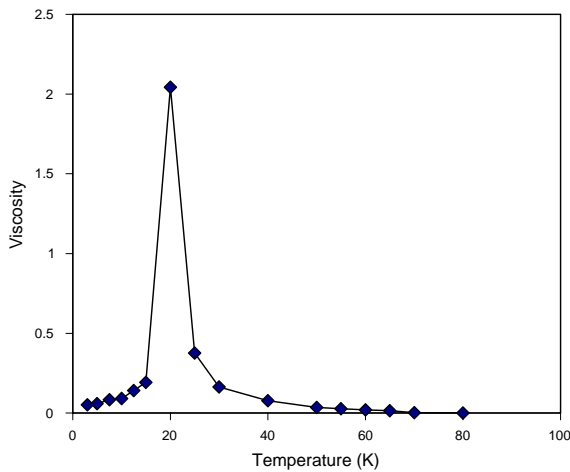


Fig. 6. Plot of the magnetic viscosity S , estimated using the data shown in Fig. 6, as a function of temperature. Lines through the data points are for visual clarity.

In summary, the high-frequency EMR results presented in this paper, along with supporting magnetic studies have shown that in FHYD, the EMR data for $T > T_s$ can be explained by the Nagata–Ishihara model for randomly oriented superparamagnetic particles. However, for $T < T_s$ (≈ 30 K), results presented here point to spin-glass like ordering of the uncompensated Fe^{3+} spins, presumably due to interparticle interactions. Presence of interparticle interaction in FHYD was also deduced by Zhao et al. from their Mössbauer studies [13] and Morup [14] has shown that dipole interaction energy in magnetic nanocomposites can lead to spin-glass ordering.

At Boise State University, this research was supported by the NSF-Idaho-EPSCoR Program

and the National Science Foundation under award # EPS-0132626 and DMR-0321051 and at West Virginia University, by the US Department of Energy (Contract #DE-FC26-02NT41594).

References

- [1] See e. g. the review by A.E. Berkowitz, K. Takano, *J. Magn. Magn. Mater.* 200 (1999) 552.
- [2] For a review of the earlier studies on ferrihydrites, see J.L. Jambor, J.E. Dutrizac, *Chem. Rev.* 98 (1998) 2549.
- [3] M.S. Seehra, V.S. Babu, A. Manivannan, J.W. Lynn, *Phys. Rev. B* 61 (2000) 3513.
- [4] M.S. Seehra, A. Punnoose, *Phys. Rev. B* 64 (2001) 132410.
- [5] A. Punnoose, T. Phanthavady, M.S. Seehra, N. Shah, G.P. Huffman, *Phys. Rev. B* 60 (2004) 054425.
- [6] M.S. Seehra, A. Punnoose, P. Roy, A. Manivannan, *IEEE Trans. Magn.* 37 (2001) 2007; A. Punnoose, M.S. Seehra, in: A. Kawamori, J. Yamauchi, H. Ohta (Eds.), *EPR in the 21st Century*, Elsevier Science, Amsterdam, 2002, pp. 162–167.
- [7] B. Martinez, X. Obradors, Ll. Balcells, A. Rouanet, C. Monty, *Phys. Rev. Lett.* 80 (1998) 181.
- [8] Yu. A. Koksharov, S.P. Gubin, I.D. Kosobudsky, G.Yu. Yurkov, D.A. Pankratov, L.A. Ponomarenko, M.G. Mikheev, M. Beltran, Y. Khodorkovsky, A.M. Tishin, *Phys. Rev. B* 63 (2000) 012407.
- [9] F. Gazeau, J.C. Bacri, F. Gendron, R. Perzynski, Yu. L. Raikher, V.I. Stepanov, E. Dubois, *J. Magn. Magn. Mater.* 186 (1998) 175.
- [10] K. Nagata, A. Ishihara, *J. Magn. Magn. Mater.* 104–107 (1992) 1571.
- [11] E.M. Chudnovsky, L. Gunther, *Phys. Rev. Lett.* 46 (1981) 211.
- [12] M.M. Ibrahim, S. Darwish, M.S. Seehra, *Phys. Rev. B* 51 (1995) 2955 (Data used in this work was taken on a dehydrated FHYD sample).
- [13] J. Zhao, F.E. Huggins, Z. Feng, G.P. Huffman, *Phys. Rev. B* 54 (1996) 3403.
- [14] S. Mørup, *Europhys. Lett.* 28 (1994) 671.